ISSN 1070-3284, Russian Journal of Coordination Chemistry, 2017, Vol. 43, No. 11, pp. 780–786. © Pleiades Publishing, Ltd., 2017.

Synthesis Characterization, Crystal Structures, and Antibacterial Activity of 8-Hydroxyquinoline-Coordinated Oxidovanadium(V) Complexes with Tridentate Hydrazone Ligands[1]

H. Y. Qian

Key Laboratory of Surface and Interface Science of Henan, School of Material and Chemical Engineering, Zhengzhou University of Light Industry, Zhengzhou, 450002 P.R. China

e-mail: hengyu_qian@126.com

Received January 18, 2017

Abstract—Two new oxidovanadium(V) complexes, [VO(L^1)(L)] (**I**) and [VO(L^2)(L)] (**II**), where L^1 and L^2 are the dianionic form of *N*'-(2-hydroxy-5-methoxybenzylidene)pivalohydrazide (H_2L^1) and *N*'-(2-hydroxy-3-methoxybenzylidene)pivalohydrazide (H_2L^2), respectively, and L is the monoanionic form of 8-hydroxyquinoline (HL), were prepared and characterized by elemental analysis, infrared and electronic spectra, and ^{1}H NMR spectra. Structures of the complexes were further confirmed by single crystal X-ray determination (CIF files CCDC nos. 1477854 (**I**), 1477856 (**II**)). H_2L^1 and H_2L^2 coordinate to the V atoms through the phenolate O, imino N, and enolate O atoms. 8-Hydroxyquinoline coordinates to the V atoms through bidentate ON donor set. The V atoms of the complexes are in octahedral coordination with the oxo group furnished the octahedral geometry. The complexes show effective antibacterial activity against *Bacillus subtilis*.

Keywords: hydrazone, oxidovanadium complex, 8-hydroxyquinoline, crystal structure, antibacterial activity

DOI: 10.1134/S1070328417110070

INTRODUCTION

In recent years, metal complexes with Schiff base ligands have received remarkable attention in biological and medicinal chemistry [1–4]. Vanadium complexes have been reported to have interesting biological activities such as normalizing the high blood glucose levels and acting as models of haloperoxidases [5–7]. In addition, vanadium complexes have shown effective antibacterial activities [8–10]. Recently, vanadium complexes with biological properties have received particular attention [11–13]. In order to explore new vanadium-based materials, in the present paper, two new oxidovanadium(V) complexes, [VOL^1L] (**I**) and [VOL^2L] (**II**), where L^1 and L^2 are the dianionic form of *N*'-(2-hydroxy-5-methoxybenzylidene)pivalohydrazide (H_2L^1) and *N*'-(2-hydroxy-3-methoxybenzylidene)pivalohydrazide (H_2L^2), respectively, and L is the monoanionic form of 8-hydroxyquinoline (HL), are presented.

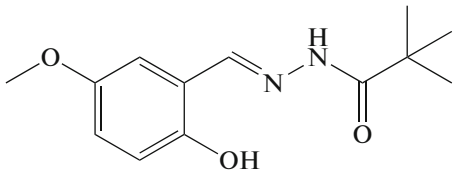

H_2L^1

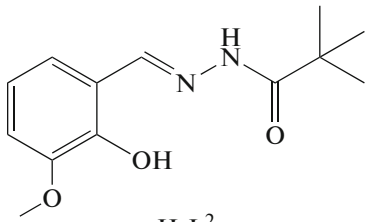

H_2L^2

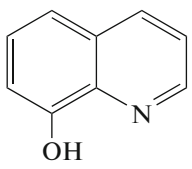

HL

[1] The article is published in the original.

EXPERIMENTAL

Materials and measurements. Commercially available 5-methoxysalicylaldehyde, 3-methoxysalicylaldehyde and pivalohydrazide were purchased from Aldrich and used without further purification. Other solvents and reagents were made in China and used as received. C, H, and N elemental analyses were performed with a Perkin-Elmer 240 elemental analyzer. Infrared spectra were recorded on a Nicolet AVATAR 360 spectrometer as KBr pellets in the 4000–400 cm^{-1} region. UV-Vis spectra were recorded on a Lambda 900 spectrometer. ^1H NMR spectra were recorded on a Bruker 300 MHz spectrometer. Thermal stability analysis was performed on a Perkin-Elmer Pyris Diamond TG-DTA thermal analyses system.

Synthesis of complex I. 5-Methoxysalicylaldehyde (0.1 mmol, 15.2 mg) and pivalohydrazide (0.1 mmol, 11.6 mg) were dissolved in methanol (15 mL). The mixture was stirred at room temperature for 30 min to give a colorless solution. To the solution was added with stirring a methanolic solution (10 mL) of 8-hydroxyquinoline (0.1 mmol, 14.5 mg) and $VO(Acac)_2$ (0.1 mmol, 26.5 mg). The mixture was further stirred at room temperature for 30 min to give a deep brown solution. After keeping the solution in air for a few days, brown block-shaped single crystals, suitable for X-ray crystal structure determination, were obtained. The crystals were isolated by filtration and dried in a vacuum desiccator containing anhydrous $CaCl_2$. The yield was 62%.

IR data (KBr; ν_{max}, cm^{-1}): 3049, 2962, 2929, 1600, 1548, 1467, 1402, 1322, 1270, 1222, 1163, 1102, 1023, 969, 834, 789, 752, 626, 554, 482. UV-Vis data in acetonitrile (λ, nm (ε, M^{-1} cm^{-1})): 242 (21230), 335 (3850), 515 (2930). ^1H NMR (300 MHz; d^6-DMSO; δ, ppm): 9.20 (s., 1H, Ar*H*), 8.55 (s., 1H, C*H*=N), 8.35 (d., 1H, Ar*H*), 7.75–7.55 (m., 3H, Ar*H*), 7.43 (s., 1H, Ar*H*), 7.09 (d., 1H, Ar*H*), 6.95 (d., 1H, Ar*H*), 6.75 (d., 1H, Ar*H*), 3.76 (s., 3H, OCH_3), 0.78 (s., 9H, CH_3).

For $C_{22}H_{22}N_3O_5V$

Anal. calcd., %:	C, 57.52;	H, 4.83;	N, 9.15.
Found, %:	C, 57.37;	H, 4.96;	N, 9.07.

Synthesis of complex II was carried out and crystallized by the same method as described for complex **I** with 5-methoxysalicylaldehyde replaced with 3-methoxysalicylaldehyde. The yield was 54%.

IR data (KBr; ν_{max}, cm^{-1}): 3054, 2966, 2929, 1602, 1557, 1503, 1479, 1443, 1383, 1330, 1263, 1218, 1096, 1033, 976, 867, 826, 752, 652, 610, 554, 498, 440. UV-Vis data in acetonitrile (λ, nm (ε, L mol^{-1} cm^{-1})): 243 (21200), 277 (9170), 347 (4120), 537 (2640). ^1H NMR (300 MHz; d^6-DMSO; δ, ppm): 9.20 (s., 1H, Ar*H*), 8.56 (s., 1H, C*H*=N), 8.12 (t., 1H, Ar*H*), 7.75 (m., 2H, Ar*H*), 7.60 (m., 1H, Ar*H*), 7.43 (q., 1H, Ar*H*), 7.22 (m., 2H, Ar*H*), 7.00 (m., 1H, Ar*H*), 3.71 (s., 3H, OCH_3), 0.78 (s., 9H, CH_3).

For $C_{22}H_{22}N_3O_5V$

Anal. calcd., %:	C, 57.52;	H, 4.83;	N, 9.15.
Found, %:	C, 57.63;	H, 4.92;	N, 9.23.

X-ray crystallography. Diffraction intensities for the complexes were collected at 298(2) K using a Bruker D8 VENTURE PHOTON diffractometer with MoK_α radiation (λ = 0.71073 Å). The collected data were reduced using SAINT [14], and multi-scan absorption corrections were performed using SADABS [15]. Structures of the complexes were solved by direct methods and refined against F^2 by full-matrix least-squares methods using SHELXTL [16]. All of the non-hydrogen atoms were refined anisotropically. Hydrogen atoms were placed in idealized positions and constrained to ride on their parent atoms. Crystallographic data for the complexes are summarized in Table 1. Selected bond lengths and angles are given in Table 2.

Supplementary material for structures has been deposited with the Cambridge Crystallographic Data Centre (CCDC nos. 1477854 (**I**), 1477856 (**II**); deposit@ccdc.cam.ac.uk or http://www.ccdc.cam.ac.uk).

Antibacterial assay. The antibacterial activity of the complexes was tested against *B. subtilis*, *S. aureus*, *E. coli*, and *P. aeruginosa* using LB medium (Luria-Bertani medium: tryptone 10 g, yeast extract 5 g, NaCl 10 g, distilled water 1000 mL, pH 7.4). The IC_{50} (half inhibitory concentration) of the test compounds were determined by a colorimetric method using the dye MTT (3-(4,5-di-methylth-iazol-2-yl)-2,5-diphenyl tetrazolium bromide).

A stock solution of the synthesized compound (1000 μg mL^{-1}) in DMSO was prepared and graded quantities of the test compounds were incorporated in specified quantity of sterilized liquid LB medium. Suspension of the microorganism was prepared and applied to 96-well assay plate with serially diluted compounds to be tested. 10 μL of tested samples at pre-set concentrations were added to wells with Penicillin as a positive reference and with the solvent control (5% DMSO) in medium and incubated at 37°C for 24 h.

After 24 h exposure, 10 μL of PBS (phosphate buffered saline 0.01 mol L^{-1}, pH 7.4) containing 4 mg mL^{-1} of MTT was added to each well. After 4 h, the medium was replaced by 150 μL DMSO to dissolve the complexes. The absorbance at 492 nm of each well was measured with an ELISA plate reader. The IC_{50} value was defined as the concentration at which 50% of the bacterial strain could survive.

Table 1. Crystallographic data and refinement parameters for complexes **I** and **II**

Parameter	Value	
	I	**II**
Mr	459.37	459.37
Crystal color, habit	Brown, block	Brown, block
Crystal size, mm^3	0.16 × 0.15 × 0.13	0.27 × 0.27 × 0.26
Crystal system	Triclinic	Triclinic
Space group	$P\bar{1}$	$P\bar{1}$
a, Å	9.3020(7)	9.6589(11)
b, Å	10.9857(8)	9.8704(11)
c, Å	11.9207(10)	11.8473(13)
α, deg	64.245(2)	90.085(2)
β, deg	76.340(3)	106.511(2)
γ, deg	85.890(2)	103.538(2)
V, $Å^3$	1065.45(14)	1050.0(2)
Z	2	2
ρ_{calcd}, g cm^{-3}	1.432	1.453
μ, mm^{-1}	0.505	0.512
F(000)	476	476
Number of unique data	3954	3852
Number of observed data ($I > 2\sigma(I)$)	2885	3538
Independent parameters	284	284
R_1, wR_2 ($I > 2\sigma(I)$)	0.0458, 0.1088	0.0299, 0.0791
R_1, wR_2 (all data)	0.0723, 0.1216	0.0331, 0.0822
Goodness of fit on F^2	1.023	1.064
Largest difference peak and hole, *e* $Å^{-3}$	0.294 and –0.202	0.186 and –0.375

RESULTS AND DISCUSSION

The hydrazone ligands H_2L^1 and H_2L^2 were prepared by the reactions of pivalohydrazide with 5-methoxysalicylaldehyde and 3-methoxysalicylaldehyde, respectively, in methanol. The two complexes were prepared by the reaction of the hydrazone ligands, 8-hydroxyquinoline and $VO(Acac)_2$ in methanol. Crystals of the complexes are soluble in DMF, DMSO, methanol, ethanol, and acetonitrile.

Molecular structures of complexes **I** and **II** are shown in Fig. 1. The V atoms in the complexes are in octahedral coordination, with the phenolate O, imino N and enalate O atoms of the hydrazone ligands, and the phenolate O atom of 8-hydroxyquinoline ligand defining the equatorial plane, and with the pyridine N atom of 8-hydroxyquinoline and the oxo group locating at the axial positions. The V atoms deviate from the least-squares plane defined by the corresponding equatorial atoms by 0.326(1) Å for **I** and 0.299(1) Å for **II**. The coordinate bond lengths in the complex are similar to those observed in vanadium complexes with hydrazone ligands [17, 18]. The distortion of the octahedral coordination can be observed from the coordinate bond angles, ranging from 74.67(8)° to 105.49(8)° for **I** and from 74.75(5)° to 100.30(7)° for **II** for the perpendicular angles, and from 154.51(8)° to 176.81(10)° for **I** and from 153.77(6)° to 175.70(6)° for

Table 2. Selected bond distances (Å) and angles (deg) for complexes **I** and **II**

Bond	*d*, Å	Bond	*d*, Å
		I	
V(1)–O(1)	1.8459(18)	V(1)–O(2)	1.9361(17)
V(1)–O(4)	1.8423(19)	V(1)–O(5)	1.580(2)
V(1)–N(1)	2.078(2)	V(1)–N(3)	2.376(2)
		II	
V(1)–O(1)	1.8558(12)	V(1)–O(2)	1.9388(11)
V(1)–O(4)	1.8511(11)	V(1)–O(5)	1.5843(13)
V(1)–N(1)	2.0903(13)	V(1)–N(3)	2.3735(14)
Angle	ω, deg	Angle	ω, deg
		I	
O(5)V(1)O(4)	102.03(10)	O(5)V(1)O(1)	98.70(10)
O(4)V(1)O(1)	105.49(8)	O(5)V(1)O(2)	99.14(9)
O(4)V(1)O(2)	88.38(8)	O(1)V(1)O(2)	154.51(8)
O(5)V(1)N(1)	99.04(10)	O(4)V(1)N(1)	154.79(9)
O(1)V(1)N(1)	84.67(8)	O(2)V(1)N(1)	74.67(8)
O(5)V(1)N(3)	176.81(10)	O(4)V(1)N(3)	75.79(8)
O(1)V(1)N(3)	84.19(8)	O(2)V(1)N(3)	78.55(7)
N(1)V(1)N(3)	82.54(8)		
		II	
O(5)V(1)O(4)	100.15(6)	O(5)V(1)O(1)	100.30(7)
O(4)V(1)O(1)	99.81(5)	O(5)V(1)O(2)	97.43(7)
O(4)V(1)O(2)	95.90(5)	O(1)V(1)O(2)	153.77(6)
O(5)V(1)N(1)	97.39(6)	O(4)V(1)N(1)	161.08(5)
O(1)V(1)N(1)	83.88(5)	O(2)V(1)N(1)	74.75(5)
O(5)V(1)N(3)	175.70(6)	O(4)V(1)N(3)	75.84(5)
O(1)V(1)N(3)	82.07(5)	O(2)V(1)N(3)	81.58(5)
N(1)V(1)N(3)	86.41(5)		

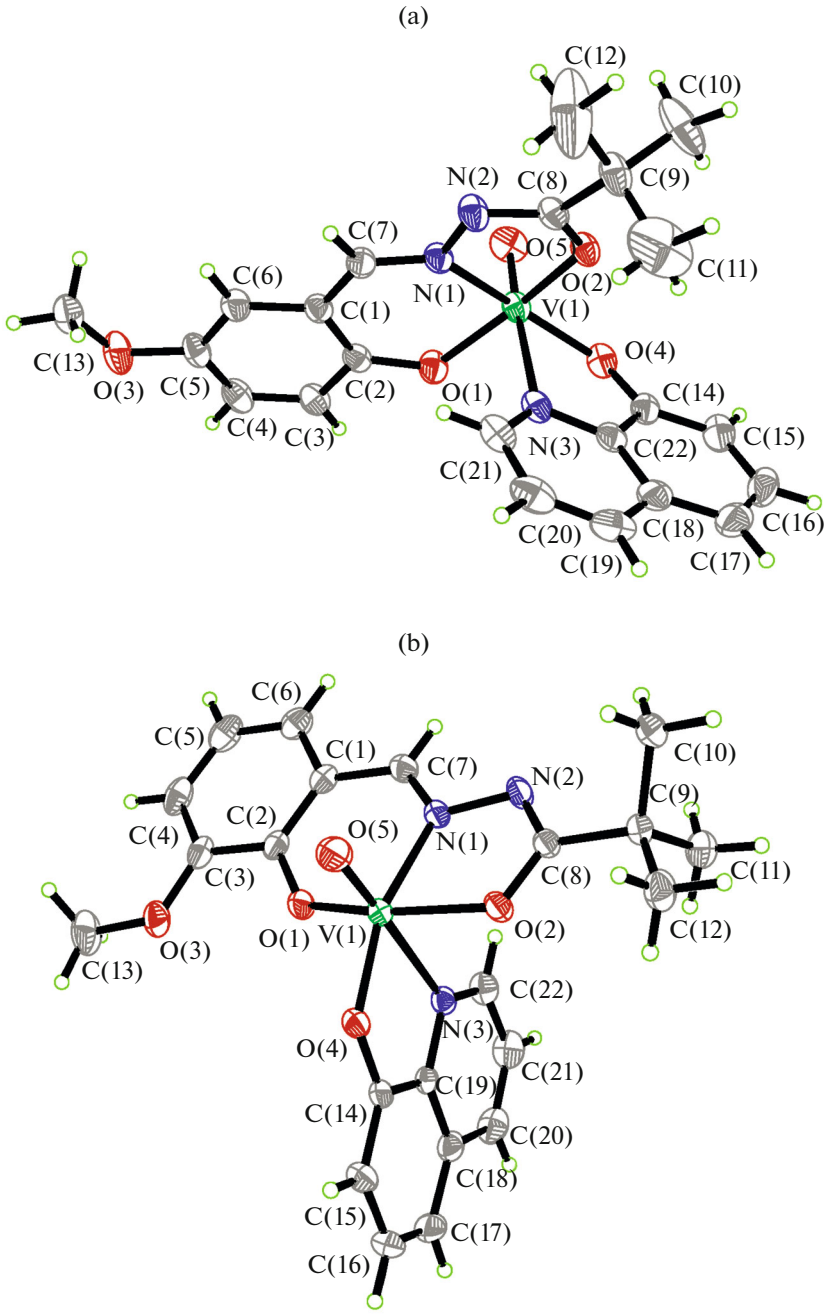

Fig. 1. Molecular structures of **I** (a) and **II** (b), showing the atom-numbering scheme. Displacement ellipsoids are drawn at the 30% probability level.

Table 3. Antibacterial results (IC_{50}, μg mL^{-1})

Compound	Gram-positive		Gram-negative	
	B. subtilis	*S. aureus*	*E. coli*	*P. aeruginosa*
I	5.72	>50	>50	>50
II	6.83	>50	>50	>50
Penicillin G	2.35	0.75	17.51	17.49

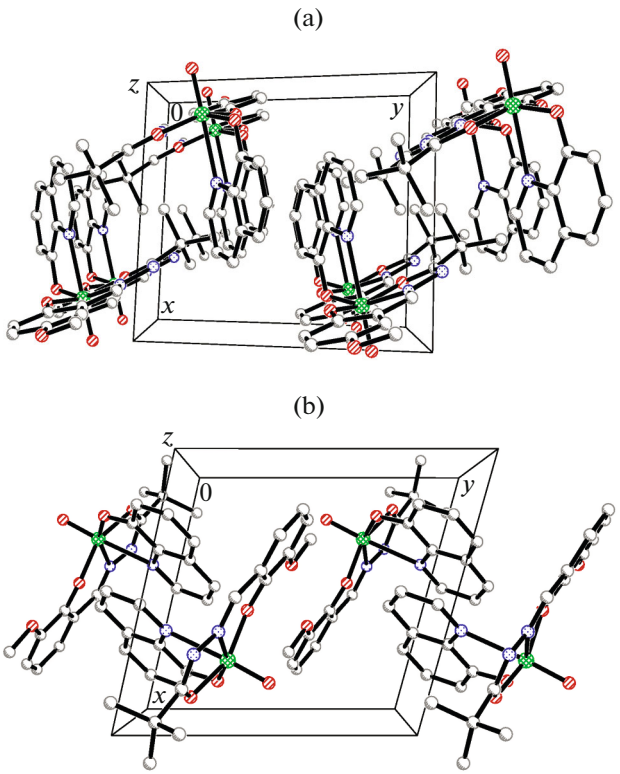

Fig. 2. Crystal packing of **I** (a) and **II** (b), viewed along the *z* axis. Hydrogen bonds are shown as dashed lines.

II for the diagonal angles. The dihedral angles between the C(1)–C(6) benzene ring and the C(14)–C(22)/N(3) aromatic plane are 76.2(3)° for **I** and 85.8(3)° for **II**. In the crystal structures of the complexes, molecules are stacked by weak π···π interactions (Fig. 2).

The ν(C=N) absorptions are observed at 1600 cm^{-1} for **I** and 1602 cm^{-1} for **II** [19]. The intense bands indicative of the C=O vibrations and the sharp bands indicative of the N–H vibrations are absent in the complexes, indicating the enolization of the hydrazone ligands. The weak peaks in the low wave numbers in the region 400–650 cm^{-1} may be attributed to V–O and V–N bonds in the complexes. Complexes **I** and **II** exhibit typical bands at 969 and 976 cm^{-1}, respectively, which are assigned to the V=O vibrations [20].

The UV-Vis spectra of the complexes were recorded in 10^{-5} mol L^{-1} in acetonitrile, in the range 200–600 nm (Fig. 3). The weak bands centered at 335 nm for **I** and 347 nm for **II** are attributed to intramolecular charge transfer transitions from the p_π orbital on the nitrogen and oxygen to the empty *d* orbitals of the metal [21]. The intense bands observed at 242 nm for the complexes are assigned to intraligand π–π* transition [21]. The bands centered at 515 nm for **I** and 537 nm for **II** are attributed to the

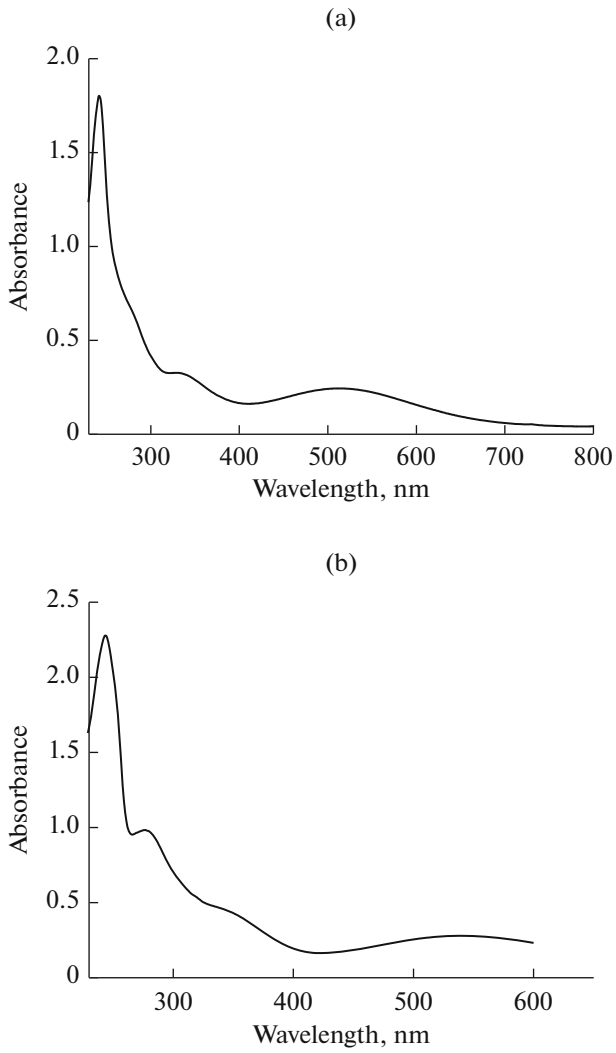

Fig. 3. UV-Vis spectrum of **I** (a) and **II** (b).

ligand-to-metal charge transfer transitions (LMCT) [22].

The complexes were screened for antibacterial activities against two Gram-positive bacterial strains (*B. subtilis* and *S. aureus*) and two Gram-negative bacterial strains (*E. coli* and *P. aeruginosa*) by MTT method. The IC_{50} values of the complexes against the bacteria are presented in Table 3. Penicillin G was tested as a reference drug. Complexes **I** and **II** exhibited effective activities against *B. subtilis*, while no activity against *S. aureus*, *E. coli,* and *P. aeruginosa*.

REFERENCES

1. Chans, G.M., Nieto-Camacho, A., Ramirez-Apan, T., et al., *Aust. J. Chem*., 2016, vol. 69, no. 3, p. 279.
2. Qureshi, F., Khuhawar, M.Y., Jahangir, T.M., et al., *Acta Chim. Slov.*, 2016, vol. 63, no. 1, p. 113.
3. Adhikary, J., Kundu, P., Dasgupta, S., et al., *Polyhedron*, 2015, vol. 101, p. 93.

4. El-Gammal, O.A., *Inorg. Chim. Acta*, 2015, vol. 435, p. 73.
5. Mba, M., Pontini, M., Lovat, S., et al., *Inorg. Chem.*, 2008, vol. 47, no. 19, p. 8616.
6. Zhang, X.A. and Woggon, W.D., *J. Am. Chem. Soc.*, 2005, vol. 127, no. 41, p. 14138.
7. Zhang, X.A., Meuwly, M., and Woggon, W.D., *J. Inorg. Biochem.*, 2004, vol. 98, no. 11, p. 1967.
8. Farzanfar, J., Ghasemi, K., Rezvani, A.R., et al., *J. Inorg. Biochem.*, 2015, vol. 147, p. 54.
9. Pawar, V., Joshi, S., and Uma, V., *Asian J. Chem.*, 2013, vol. 25, no. 8, p. 1497.
10. Sheikhshoaie, I., Ebrahimipour, S.Y., Lotfi, N., et al., *Inorg. Chim. Acta*, 2016, vol. 442, p. 151.
11. He, M., Jiao, Q.Z., Chen, X.F., et al., *Chin. J. Inorg. Chem.*, 2015, vol. 31, no. 8, p. 1590.
12. Ren, J.Q., Jiao, Q.Z., Wang, Y.N., et al., *Chin. J. Inorg. Chem.*, 2014, vol. 30, no. 3, p. 640.
13. Zhao, X.L., Chen, X.F., Li, J., et al., *Polyhedron*, 2015, vol. 97, p. 268.
14. *SMART (version 5. 624) and SAINT (version 6.04), Programs Using the Windows NT System*, Madison: Bruker AXS Inc., 2001.
15. Sheldrick, G.M., *SADABS, Program for Empirical Absorption Correction of Area Detector*, Göttingen: Univ. of Göttingen, 1996.
16. Sheldrick, G.M., *Acta Crystallogr., Sect. A: Found. Crystallogr.*, 2008, vol. 64, no. 1, p. 112.
17. Qu, D., Niu, F., Zhao, X., et al., *Bioorg. Med. Chem.*, 2015, vol. 23, no. 9, p. 1944.
18. Li, L.-X., Sun, Y., Xie, Q., et al., *Chin. J. Inorg. Chem.*, 2016, vol. 32, no. 2, p. 369.
19. You, Z.-L., Xian, D.-M., and Zhang, M., *CrystEngComm*, 2012, vol. 14, no. 21, p. 7133.
20. Sangeetha, N.R., Kavita, V., Wocadlo, S., et al., *J. Coord. Chem.*, 2000, vol. 51, no. 1, p. 55.
21. Asgedom, G., Sreedhara, A., Kivikoski, J., et al., *Dalton Trans.*, 1996, vol. 1, no. 1, p. 93.
22. Sarkar, A. and Pal, S., *Polyhedron*, 2006, vol. 25, no. 7, p. 1689.